Environ Monit Assess (2026) 198:606
https://doi.org/10.1007/s10661-026-15436-5

RESEARCH

Assessing the air quality performance of urban garden designs: an integrated ENVI-met modeling and field measurement study in Guelma, Algeria

Rayen Bechlem · Fatima Zahra Djouad · Hocine Boudjehem · Hana Salah-Salah

Received: 29 November 2025 / Accepted: 8 May 2026 / Published online: 19 May 2026

Abstract Urban air quality degradation, driven by intensified urbanization and traffic, presents a critical public health challenge in most cities worldwide, such as Guelma, Algeria, where concentrations of fine particulate matter ($PM_{2.5}$, PM_{10}) and carbon dioxide (CO_2) often exceed health standards. This study evaluates the efficacy of conventional greening by suggesting that the air purification potential of public gardens may be limited by suboptimal initial design. It is an exploratory modeling framework to propose a shift from qualitative landscaping to quantitative, performance-driven biophilic design. By simulating six parameterized intervention scenarios, this research indicates that simplistic canopy densification may be an insufficient strategy under high pollutant loads. Based on a specific summer field campaign and a limited temporal scope, the results identify a proposed design configuration protocol, where significant pollutant mitigation is achieved by a specific arrangement: a 60% urban forest index composed of high-efficiency species (*Platanus* × *acerifolia*, *Acer saccharinum*, *Quercus* spp.), combined with a 10% shrub layer and 40% grass cover to form a multilayered filter. This vegetative system is integrated with complementary engineered systems: linear water features covering 15% of the surface for particle wash-down, soil engineered to an aerodynamic roughness length (z_0) of 0.15 m across 65% of the site to enhance deposition, and pollutant-absorbing paving on 20% of the surface. This study suggests that enhancing the functional efficiency of urban gardens requires precise, multimechanism integration of biomass, water, and engineered surfaces, providing an exploratory framework for designing public spaces as potential infrastructure for sustainable air quality improvement.

Keywords Green space · Particulate matter · CO_2 · ENVI-met · Biophilic design · NDVI

Supplementary Information The online version contains supplementary material available at https://doi.org/10.1007/s10661-026-15436-5.

R. Bechlem (✉) · H. Boudjehem
Laboratory of Civil Engineering and Hydraulics, Department of Architecture, University 8 Mai 1945, Guelma, Algeria
e-mail: bechlem.rayen@univ-guelma.dz; rayen.bechlem@gmail.com

H. Boudjehem
e-mail: boudjehem.hocine@univ-guelma.dz

F. Z. Djouad · H. Salah-Salah
Laboratory of "Architecture, Sustainability and Resilient Cities", Department of Architecture, University 8 Mai 1945, Guelma, Algeria
e-mail: djouad.fatimazahra@univ-guelma.dz

H. Salah-Salah
e-mail: salahsalah.hana@univ-guelma.dz

Introduction

The rapid expansion of urban areas, driven by population growth and industrial activity, places considerable stress on urban environments, often leading to the degradation of air quality (Ramírez et al., 2017; Liu et al., 2021; Rodrigues et al., 2021). A critical manifestation of this issue is the frequent exceedance of health-based standards for atmospheric pollutants, particularly particulate matter (PM), in cities worldwide. The World Health Organization (WHO) has reported that the global population-weighted annual mean concentration of $PM_{2.5}$ remains dangerously high, approximately six times above its updated guideline of 5 μg/m^3 (Godwin et al., 2015; H. Liu et al., 2017; Rodrigues et al., 2021; Wang et al., 2022). Concurrently, the continuous rise in carbon dioxide (CO_2) emissions, the primary greenhouse gas, exacerbates climate change and contributes to urban air pollution profiles, with global projections reaching record levels (Muñoz-Pizza et al., 2020; Du et al., 2021; Dong et al., 2023). This persistent dual challenge of particulate pollution and elevated CO_2 concentrations represents a pressing environmental and public health crisis for metropolitan regions (Bouznit & Pablo-Romero, 2016; Shi et al., 2022).

Vegetation and other biophilic elements serve as a crucial natural filter in urban environments, directly mitigating airborne particulate matter ($PM_{2.5}$) through two primary mechanisms: the surface adsorption of particles onto leaves and the alteration of airflow patterns to promote deposition (Du et al., 2021; Ge & Zhang, 2022; Bechlem et al., 2025). The movement and eventual capture of these particles within plant canopies are governed by gravitational settling and concentration gradients (H. Liu et al., 2017; Muñoz-Pizza et al., 2020; Villani et al., 2021). The efficacy of this filtration is highly dependent on vegetation structure. Specifically, dense foliage characterized by a high leaf area density and a low crown base height has been demonstrated to significantly enhance PM removal (Khaleghi et al., 2011; Vigevani et al., 2022). This principle extends to the landscape scale, where strategically placed vegetative barriers can effectively reduce PM concentrations in downwind areas (Du et al., 2021; Dong et al., 2023; Acierno & Coppola, n.d.). To maximize air quality benefits, the design of public green spaces must move beyond simple greening and prioritize multilayered vegetation structures. Arrangements that combine trees, shrubs, and groundcover are most effective; those with a well-developed shrub layer capture the most PM at capturing $PM_{2.5}$ and PM_{10}, underscoring the importance of intentionally structured complexity in urban landscape design (Buccolieri et al., 2020; Wang et al., 2022; Dong et al., 2023; Gebreyesus et al., 2024).

Particulate matter dynamics in urban areas are governed by processes across multiple scales. At the microscale, surface properties are a fundamental control. Soil texture dictates dust emission potential, where cohesive clay-rich soils resist erosion, while noncohesive sandy soils are highly prone to particulate resuspension (VanOort et al., 2008; Aimar et al., 2012). Similarly, material characteristics govern PM retention; porous and electrostatically charged wood surfaces effectively capture particles, whereas smooth, nonporous materials like metal facilitate only temporary deposition, leading to easy resuspension (Sjöblom et al., 2017; Vigevani et al., 2022).

These microscale interactions are contextualized and driven by macro-scale urban forms. Land-use composition (the spatial arrangement of residential, commercial, and industrial zones) shapes traffic patterns, a primary source of $PM_{2.5}$ PM_{10} from exhaust and nonexhaust emissions (Fisher et al., 2006; Tarek & Ouf, 2021). Urban compactness can intensify this source by concentrating traffic flows and causing congestion (Brulfert et al., 2005; Hu, 2017). Furthermore, the geometry of the urban fabric, such as street canyons oriented parallel to prevailing winds, can create a wind channeling effect that traps emissions and elevates ground-level pollutant concentrations (Ramirez et al., 2017; Jin et al., 2023). Within the Algerian context, these challenges are exacerbated by morphological configurations such as canyon-like streets that have been shown to restrict ventilation and trap pollutants at the pedestrian level (Khellaf et al., 2025). Such localized environmental stressors highlight the need to move beyond traditional, qualitative landscaping and explore more technical, performance-driven interventions.

Consequently, the objective of this research is to investigate the air purification potential of public gardens in Guelma through the exploration of parameterized biophilic design scenarios. By utilizing a predictive modeling framework, this study evaluates various combinations of high-efficiency vegetation layers, integrated water features, and engineered surfaces to identify optimized protocols for pollutant mitigation. Rather than a purely aesthetic approach, this study seeks to provide a theoretical and practical basis for reimagining public garden as an active environmental infrastructure capable of responding to the specific air quality demands of the Mediterranean urban fabric.

Case study

The global trend of urban environmental degradation is mirrored in Guelma (Ramdane et al., 2025), a verdant, mountainous city in northeastern Algeria. The city is experiencing a marked exacerbation of concerns regarding air quality, driven by intensified urbanization and industrial expansion. Data from the National Observatory for Environment and Sustainable Development indicate that ambient levels of fine particulate matter (PM) and carbon dioxide (CO_2) have risen significantly since the 2000 s, exceeding the World Health Organization's (WHO) annual average guidelines by 2023. Furthermore, a dramatic increase in the number of vehicles over the past decade (Smieszek et al., 2021; Bechlem et al., 2024) has compounded issues such as traffic congestion and associated atmospheric pollution. These anthropogenic suspended particles originate primarily from a variety of sources, including road traffic, industrial processes, and commercial activities, as well as residential heating and cooking (Gehanno et al., 2020).

Public gardens serve as vital recreational and ecological refuges within dense urban areas, a role particularly critical during warm climatic periods (Bechlem et al., 2025). In the city of Guelma, these green spaces exhibit significant heterogeneity in their design, including their adjacency to traffic arteries, internal vegetation structure, and integration within the urban matrix. These variations necessitate a systematic investigation into how specific design attributes influence microclimatic conditions and air quality. Therefore, this study aims to quantitatively assess the functional efficacy of different public garden designs in Guelma for mitigating concentrations of $PM_{2.5}$, PM_{10}, and CO_2 at the microscale. The central research question is how do the composition and spatial configuration of biophilic elements within a public garden's design determine its efficacy in reducing ambient $PM_{2.5}$, PM_{10}, and CO_2 concentrations?

This research is predicated on the hypothesis that the efficacy of biophilic design in capturing air pollutants is a quantifiable function of its specific characteristics. Employing a controlled, bottom-up simulation approach, this study systematically modulates key variables including vegetation type and density, green coverage ratio, and the configuration of blue infrastructure and natural soils. This methodology within this conditions enables the precise isolation and quantification of their individual and synergistic impacts on the sequestration of $PM_{2.5}$, PM_{10}, and CO_2. The ultimate objective is to develop an optimized model for biophilic design that yields evidence-based guidelines for maximizing the air quality enhancement function of urban green spaces.

Research methodology and materials

This study employs an integrated bottom-up methodology to quantify the impact of urban garden design on ambient air quality, aligning with contemporary research on biophilic urbanism (Djouad, 2021; Beatley & Newman, 2013). The research is structured as a case study of three public gardens in Guelma, selected based on criteria of vegetation cover, traffic intensity, and frequency of use. The methodology comprises three sequential phases (Fig. 1). The initial phase involves a detailed site characterization through the calculation of landscape configuration indices (e.g., biophilic ratios) and an in situ environmental monitoring campaign measuring $PM_{2.5}$ and PM_{10} concentrations. Subsequently, these empirical data are used to calibrate and validate a high-fidelity ENVI-met microclimate model. The validated model is then employed to simulate CO_2 fluxes (sequestration and emission). In the final phase, the calibrated model is used to develop and test optimized design scenarios, with the goal of identifying configurations that maximize the capture and sequestration of $PM_{2.5}$, PM_{10}, and CO_2.

This approach, which integrates spatial analysis, field monitoring, and computational simulation, resonates with methodologies used in recent localized studies of biophilic design, such as the work of Ristianti et al. (2024), which combined spatial analysis with in situ particulate matter monitoring.

Spatial and biophilic analysis of the case study

Three public gardens in Guelma were selected as case studies based on criteria including the distinct presence of biophilic design elements and their variable

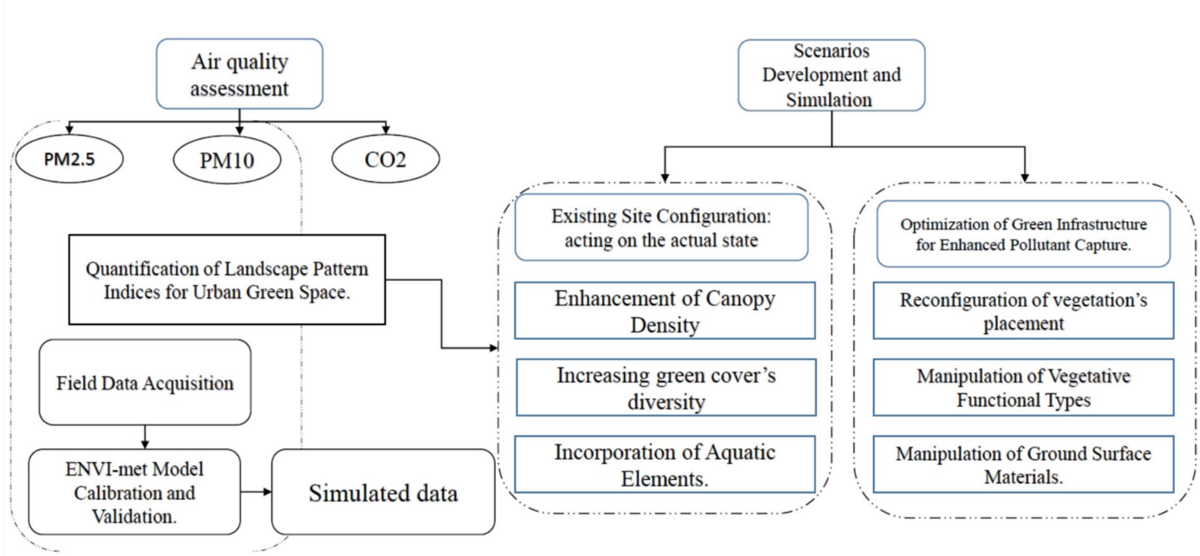

Fig. 1 Research methodology. Source: authors (2025)

proximity to vehicular traffic (Bouhallit et al., 2024). To quantitatively characterize the design and context of each site, key biophilic and spatial ratios were derived and are presented in Table 1. A complementary qualitative assessment of spatial and architectural quality was conducted through systematic field surveys (Zahra et al., 2025). This evaluation documented critical structural components of the urban fabric (Hu, 2017; Bechlem et al., 2025), with a specific focus on urban form, vegetation structure, surface material properties, and the implementation of biophilic features (Boulekbache-Mazouz, 2008).

Field measurement protocol for air quality

Air quality was assessed through a systematic in situ monitoring campaign across the three selected public gardens (Redondo Bermúdez et al., 2023). The campaign was conducted over four representative summer days in June, with measurements recorded at 2-h intervals at five pre-established stations within each garden. The placement of these stations was determined by multiple site-specific factors, including orientation, substrate type, vegetation density and typology, and proximity to vehicular traffic arteries. Particulate matter concentrations ($PM_{2.5}$ and PM_{10}) were measured using a PCE-MPC 20 Air Sampler, which provides data with a resolution in μg/m^3. This instrument is specifically designed for quantifying ambient concentrations of suspended fine particulate matter. The device delivers precise numerical data and features a color-coded display for rapid qualitative assessment against established air quality indices, enabling immediate interpretation of concentration thresholds during the fieldwork.

ENVI-met model configuration and validation for pollutant dispersion

The ENVI-met software, a three-dimensional microclimate model based on computational fluid dynamics, was employed to simulate urban environmental conditions (J. Liu et al., 2021). This tool applies the fundamental laws of fluid dynamics and thermodynamics to simulate a range of microclimatic parameters, including air temperature, humidity, wind flow, radiation, and pollutant dispersion. For this study, the simulation domain was configured as a standard $50 \times 50 \times 30$ grid with a spatial resolution of $5\ m \times 5\ m \times 3\ m$ per cell.

The simulation was designed to model the dispersion of particulate matter (PM) in Guelma, Algeria (36.46° N, 7.43° E) over a 14-h diurnal cycle starting at 07:00 local time (Table 1). Initial meteorological conditions, sourced from Meteonorm data, were configured to represent a scenario of limited

Table 1 Input data for the ENVI-met model

Start and duration of mode run	Input data
Start date of simulation	06–09/06/2024-
Start time	07:00:00
Total simulation times (hours)	14
Initial meteorological conditions	Meteonorm file
Wind speed at 10 m heigh (m/s)	2
Wind direction (deg)	90
Roughness length at measurement site	0.01
Min and max temperature of atmosphere (°C)	17 min–41.7 max
Min and max relative humidity in 2 m (%)	17 min–75.5 max
Building temperature	25 °C (constant)
Output intervals	2 h
Receptors and buildings (min)	30
All other files (min)	60
Name of location	Guelma, Algeria
Latitude (deg, + N, − S)	36.46
Longitude (deg, − W, + E)	7.43
Time zone	CET/UTC + 1
Time reference longitude	15
Type of pollutants	Particulate matter
Particle density (g/cm^3)	1.00
Road type	Inner-urban road
Daily traffic volume (DTV)	800,000 vehicles per 24 h
Number of lanes	2
Passenger cars (PCs), light duty vehicles (LDVs), heavy duty vehicles (HDVs), motorcycles (MCs), urban buses, coaches	37%, 5%, 2.5%, 15.5%, 20%, 15%

atmospheric dispersion. This was characterized by light easterly winds (2.0 m/s at 10 m height) and a low surface roughness length (0.01 m), conditions that inhibit pollutant advection and dilution. The significant diurnal temperature range (17.0–41.7 °C) and relative humidity fluctuation (17.0–75.5%) reflect a semiarid summer climate, promoting strong daytime convective mixing. Model simplifications included a constant building temperature (25.0 °C) to streamline near-field dynamics, and PM was simulated with a standardized density of 1.00 g/cm^3. Receptor outputs were configured at 30-min intervals to capture high-resolution temporal data on ground-level concentrations, framing an analysis focused on peak exposures under poor ventilation potential (Table 1).

Traffic emission sources were configured based on data obtained from the Transport Administration of Guelma. Emissions were explicitly modeled as line sources along the main roads adjacent to the study sites using ENVI-met's Traffic Toolbox (Table 1). Emission factors for relevant pollutants (g/km per vehicle) were adopted from the ENVI-met database. CO_2 emissions are calculated internally by the model based on vehicle type and default fuel consumption assumptions. No anthropogenic respiration sources were explicitly modeled, as ENVI-met does not include this process by default and its contribution at the microscale was considered negligible relative to traffic emissions. The atmospheric background CO_2 concentration was set to 400 ppm in all simulations, consistent with typical open urban environments. This value was configured in the ENVI-met "Atmospheric CO_2 Background" settings within the ENVI-guide interface.

To ensure the reliability of the ENVI-met simulations, a systematic calibration was performed by adjusting the inflow boundary conditions specifically wind speed and initial pollutant concentrations to match the meteorological conditions recorded during the field campaign in the Guelma gardens. Validation of $PM_{2.5}$ was conducted using a temporal subset of the field data that was maintained independently from the initial model forcing parameters, ensuring that the high statistical agreement reflects the model's predictive capacity rather than a simple reproduction of input data. Statistical performance was assessed using the root mean square error (RMSE) and the coefficient of determination (R^2), providing a quantitative measure of the simulation's ability to track diurnal fluctuations.

This rigorous approach used a set of performance metrics essential in environmental modeling to certify the model's accuracy. The ENVI-met model was validated through a comparative statistical analysis between in situ measured fine particle concentrations and simulated values. This process employed established performance metrics to rigorously evaluate model accuracy.

A primary metric was the root mean square error (RMSE), which quantifies the average magnitude of the prediction errors. A lower RMSE value indicates a closer agreement between the simulated and observed data, thereby ensuring the model's predictive accuracy.

$$\mathrm{RMSE} = \sqrt{\left\{ \frac{1}{n} \sum_{\{i=1\}}^{\{n\}} (yi - \widehat{yi})^2 \right\}}$$

Mean absolute error (MAE): This provides a more direct assessment of the mean error that is less sensitive to outliers, acting as a reliable complement to RMSE.

$$\mathrm{MAE} = \frac{1}{n} \sum_{\{i=1\}}^{\{n\}} \left| yi - \widehat{yi} \right|^2$$

The coefficient of determination (R^2): This metric evaluates the proportion of variance in the measured data explained by the model. An R^2 value approaching 1 indicates a strong linear relationship and high predictive performance.

Index of agreement (d) (Willmott et al., 1985): This dimensionless statistic measures the degree of model-prediction agreement, standardized by the potential error. A value near 1 denotes near-perfect concordance between simulated and observed trends.

$$d = \frac{1}{n} \left\{ \sum_{\{i=1\}}^{\{n\}(P_i - M_i)^2} \right\} \left\{ \sum_{\{i=1\}}^{\{n\}\left(\left|P_i - ^{-}\{M\}\right| + \left|M_i - ^{-}\{M\}\right|\right)^2} \right\}$$

Design of mitigation scenarios

This study employs a prospective modeling protocol to quantify the impact of biophilic infrastructure on the mitigation of atmospheric pollutants ($PM_{2.5}$, PM_{10}, and CO_2). The protocol is structured around two strategic axes, each comprising three parameterized scenarios.

The first axis, "enhancement of existing vegetation," focuses on augmenting the site's inherent vegetative capital:

Scenario 1: Increased green cover density: evaluates the impact of quantitatively increasing existing plant biomass.

Scenario 2: Diversified green cover: explores the effect of enhancing ecological complexity by introducing diverse plant species and strata (e.g., trees, shrubs, turf).

Scenario 3: Integration of water features: models the introduction of water bodies or wetland areas to diversify pollutant capture pathways (Fig. 1).

The second axis, "optimization of biophilic design components," investigates targeted modifications to the landscape's physical and aerodynamic properties.

Scenario 4: Reconfiguration of vegetation placement: modifies the spatial arrangement of vegetation to optimally interact with prevailing wind flows.

Scenario 5: Modification of vegetation type: involves substituting species to select those with foliar morphologies and architectures most effective for particulate retention.

Scenario 6: Modification of ground surface materials: focuses on altering pavement and soil properties to influence surface thermodynamics and hydrology, thereby affecting pollutant dispersion and deposition (Table 2).

Scenario implementation and ENVI-met parameterization

To ensure the scientific reproducibility of the biophilic interventions, the transition from the baseline configuration to the proposed scenarios was executed through systematic reparameterization of the ENVI-met Albero and Database systems. Each scenario was defined by a specific set of thermophysical and biological constants, as summarized in Table 2, rather than by qualitative vegetation descriptors.

Table 2 The three gardens' actual situation and the proposed one

Gardens	Actual situation	The proposed	
Kabailia Lakhder Garden	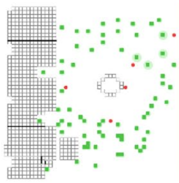 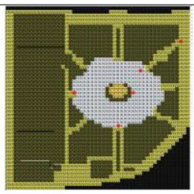 Vegetation type : Washingtonia palm, a palm tree with a large trunk.	To meet the 60% Urban Forest Index goal, the total projected surface area of the tree canopy must be increased to 5062.5828 m²	Vegetation changed type to: London Plane (Platanus x acerifolia / Platanus orientalis), Silver Maple, Oak Species.
Les frères Boulmokh Garden	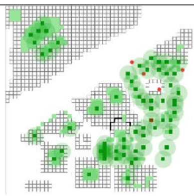  Vegetation type: Himalayan Fir pin tree, Washingtonia palm, The common ash tree.	To meet the 60% Urban Forest Index goal, the total projected surface area of the tree canopy must be increased to 5758.33 m²	Vegetation changed type to: London Plane (Platanus x acerifolia / Platanus orientalis), Silver Maple, Oak Species.
Ben Mihoub Hassen	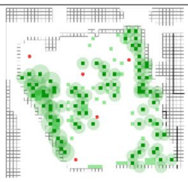 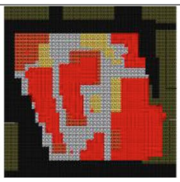 Vegetation type: Himalayan Fir pin tree, Washingtonia palm.	To meet the 60% Urban Forest Index goal, the total projected surface area of the tree canopy must be increased to 3542.981m².	Vegetation changed type to: London Plane (Platanus x acerifolia / Platanus orientalis), Silver Maple, Oak Species.

Vegetation substitutions, including the replacement of Washingtonia palms with *Platanus × acerifolia*, were modeled by adjusting the vertical profiles of leaf area density (LAD) across five vertical nodes. These adjustments were configured to represent the structural characteristics of each species within the urban canopy layer. Biological parameters, including stomatal resistance and leaf transmissivity, were assigned values consistent with the physiological and radiative properties of Mediterranean species.

The spatial configuration of vegetation within each garden was quantified using established biophilic indicators. The urban forest index was applied to regulate canopy closure at a target threshold of 60%, while the ecological landscaping plot ratio (Rg) was employed as a weighted metric for assessing potential CO_2 concentration dynamics. Material modifications, such as the integration of shallow water bodies and porous concrete pavements, were defined by their physical properties, including specific heat capacity, albedo, and aerodynamic roughness length (z_0). This level of parameterization ensures that the simulated microclimatic and air quality outcomes are attributable to reproducible, physically based emission and dispersion processes.

Results

Simulated CO_2 concentrations

It is important to note that while the model outputs for $PM_{2.5}$ and PM10 were validated against in situ measurements from the field campaign, CO_2 concentrations were not directly observed. Accordingly, the CO_2 results presented herein are derived from simulations that rely on the internal biogenic and dispersion algorithms of the modeling software. Boundary conditions for CO_2 were initialized using a standardized urban background concentration 400 ppm and were subsequently modulated to incorporate local traffic emission sources as characterized by the Guelma Transport Administration. These simulations should therefore be interpreted as scenario-based estimates that illustrate the relative performance of the proposed biophilic interventions. They are not intended to represent absolute flux accounting or verified carbon sequestration but rather to provide an exploratory assessment of potential concentration dynamics under specified assumptions. Crucially, it is necessary to distinguish between the various mechanisms influencing CO_2 in this study; the results primarily reflect concentration changes driven by aerodynamic dispersion and localized microclimatic shifts, rather than immediate biological uptake or long-term sequestration. Given that these values were derived from modeling assumptions without direct field validation, they are presented as an exploratory assessment of potential concentration dynamics rather than absolute flux accounting. The actual performance of these interventions in terms of verified carbon sequestration would require long-term monitoring of vegetative maturation and biomass accumulation, which falls outside the temporal scope of this diurnal simulation.

The simulated CO_2 time profiles in the three gardens indicate that local emission patterns and aerodynamic constraints have a greater influence on localized concentration dynamics than the potential carbon sequestration capacity of vegetation (Table 3). It should be noted that the Kabailia Lakhder Garden had the most favorable atmospheric conditions, with the lowest average simulated concentration (378.61 ppm) and a maximum peak of only 399.00 ppm. This suggests that its spatial configuration facilitates effective atmospheric dispersion and minimizes the accumulation of anthropogenic emissions. Conversely, the Les Frères Boulmokh Garden, located near busy traffic arteries, showed the highest temporal variability, reaching a maximum concentration of 409.00 ppm during rush hour. This highlights the impact of localized and intense sources of pollution on the garden's microclimate. It is worth noting that the Ben Mihoub Hassen Garden recorded the highest average CO_2 concentration (390.92 ppm), despite having the highest biomass density. A detailed temporal analysis (see supplementary file) reveals that the dense canopy, although conceptually intended for sequestration, likely contributes to restricting air circulation and creating "stagnation zones," thus preventing the dilution of high background emissions. These results are supported by the data collected every 2 h (Table 3).

The values that exceeded 400 ppm represent localized, microscale concentrations within and immediately adjacent to dense vegetation patches, particularly during periods of low wind speed and high atmospheric stability. Under such conditions, reduced vertical mixing and canopy-induced stagnation can lead to local CO_2 accumulation from the combined effects of traffic emissions during peak hours contributing to local CO_2 buildup, particularly in areas with limited ventilation, and plant respiration, which in ENVI-met is modeled as a continuous source (with temperature dependence), accumulating under stagnant nighttime conditions when photosynthetic uptake is absent. As CO_2 was not measured in situ, these findings serve to illustrate the hypothetical influence of biophilic design on air quality trends under specified modeling assumptions.

Spatial and biophilic characterization via green indices

The capacity of urban green spaces to mitigate atmospheric pollution is largely determined by the extent and configuration of their functional biomass. This study utilizes structural landscape indices to quantitatively characterize the three case study gardens. The urban forest index, defined as the ratio of tree canopy

Table 3 Technical proprieties of the simulated scenarios

Case study and scenario	Parameter/intervention	Technical properties (ENVI-met configuration)	Implementation method and reproducibility metrics
Baseline (all sites)	Existing vegetation	Washingtonia palm: height 12 m; stem height 8 m; crown height 4 m; crown diameter 3.5 m; LAD 0.3 m^2/m^3; leaf albedo 0.25; transmissivity 0.30; stomatal resistance 400 s/m; root depth 1.0 m; fractional coverage 0.7	Represents the "actual situation" low-filtration canopy profile with sparse foliage and low aerodynamic roughness
Proposed scenarios (general)	Optimized species	*Platanus × acerifolia*/*Quercus* spp.: height 15–20 m; stem height 4–6 m; crown diameter 8–12 m; LAD 1.1–2.5 m^2/m^3 (vertical profile distributed across 5 nodes); leaf albedo 0.15–0.20; transmissivity 0.15–0.25; stomatal resistance 200–300 s/m; root depth 1.5 m; fractional coverage 0.9	High-density leaf surface area configured for maximum dry deposition of particulate matter. LAD profile optimized for $PM_{2.5}$ and PM10 capture based on species-specific deposition velocities
	Shrub and grass layer	*Buxus sempervirens*/*Lavandula angustifolia*: height 1.0–1.5 m; LAD 0.8–1.2 m^2/m^3 (uniform vertical distribution); leaf albedo 0.15–0.18; transmissivity 0.20; stomatal resistance 300 s/m; root depth 0.5 m; fractional coverage 0.8. Soil layer: roughness length (z_0) 0.01 m; albedo 0.15; volumetric water content 0.3 m^3/m^3; thermal conductivity 1.5 W/(m·K); heat capacity 2.0×10^6 J/(m^3·K)	Modeled as porous windbreaks and permeable cooling surfaces with specific aerodynamic resistance parameters
Kabailia Lakhder Garden	Urban forest index 60% and shrub optimization	Canopy expansion: total canopy area 5062.58 m^2 (33 new trees); canopy closure 60%; mean tree spacing 8 m. Shrub layer: total shrub area 2531.29 m^2 (30% ground cover); shrub height 1.2 m; LAD 1.0 m^2/m^3. Soil amendment: topsoil layer depth 0.3 m; organic matter content 5%; albedo 0.12	Ecological plot ratio (Rg) 6.74 (moderate). Isolation index (Fi) 0.022. Trees arranged in staggered grid pattern to maximize canopy interception
	Vertical greening	*Hedera helix*: height 6 m (wall-attached); LAD 0.5 m^2/m^3 (foliage density); leaf albedo 0.18; transmissivity 0.10; stomatal resistance 350 s/m; root depth 0.3 m (base); substrate depth 0.15 m	Applied as biological filtration mats on windward boundary walls (northern and western facades). Modeled as green wall module with integrated substrate layer

Table 3 (continued)

Case study and scenario	Parameter/intervention	Technical properties (ENVI-met configuration)	Implementation method and reproducibility metrics
Les Frères Boulmokh	Urban forest index 60% and cluster optimization	Canopy expansion: total canopy area 5758.33 m^2 (23 new trees); canopy closure 60%; cluster density 4–6 trees per cluster; intercluster spacing 15 m. LAD optimization: PM10-optimized profile with peak LAD (2.2 m^2/m^3) at 8–12 m height; $PM_{2.5}$-optimized foliage density (1.5 m^2/m^3) at 4–6 m height	Rg 13.19 (High). Fi 0.008. Connected groves aligned with prevailing wind direction (northwest) to maximize pollutant interception while maintaining ventilation corridors
	Water features (Scenario 03)	Material type: default ENVI-met fountain (0000W2). Surface properties: albedo 0.05; emissivity 0.98; roughness length (z_0) 0.0002 m. Physical parameters: water depth 0.5 m; specific heat capacity 4182 J/(kg·K); thermal conductivity 0.6 W/(m·K); density 998 kg/m^3; initial temperature 18 °C	Area 600 m^2 (7.11% of site). Configured as shallow water body with continuous circulation. Positioned downwind of primary emission sources for thermal stratification effects
Jardin Ben Mihoub	Urban forest index 60% and diversity boost	Canopy expansion: total canopy area 3542.98 m^2; canopy closure 60%; species mix 40% *Betula pendula*, 30% *Platanus*, 30% *Quercus*. *Betula pendula* properties: height 12–15 m; LAD 1.8 m^2/m^3 (PM-adherent surface morphology); leaf albedo 0.16; transmissivity 0.18; stomatal resistance 250 s/m; trichome density: high (specified for PM adhesion)	Rg 11.96 (high). Deviation index (Pd) 0.16 (centralized placement with radial distribution from core). Species selected for documented PM capture efficiency based on micromorphological traits
	Soil and pavement (Scenario 04)	Permeable pavement: material: porous concrete; layer depth 0.15 m; albedo 0.20; emissivity 0.90; thermal conductivity 1.2 W/(m·K); heat capacity 1.8×10^6 J/(m^3·K); permeability 0.5 (fraction); roughness length (z_0) 1.2 m. Subbase layer: depth 0.3 m; porosity 0.25; saturation 0.3	Increased surface roughness configured to enhance turbulent dispersion in identified hotspot areas (intersection of pedestrian pathways). Permeable fraction allows evaporative cooling and reduced runoff

area to total garden area, serves as a primary indicator of pollutant interception potential. The calculated UFCI values reveal significant disparities, with Les Frères Boulmokh Garden exhibiting the highest coverage (36.32%), followed by Ben Mihoub Hassen Garden (30.38%) and Jardin Kabailia Lakhder (21.75%) (Table 4).

Analysis of the lower vegetation strata and the total vegetation ratio (TVR) allows for further differentiation between the sites. The Ben Mihoub Hassen Garden has the highest TVR (25.4%), a value mainly due to its shrub cover (14.4%). In comparison, the Kabailia Lakhder Garden recorded a TVR of 4.5%, consisting of 1.96% herbaceous cover and 2.56% shrub cover. These measurements reflect the predominance of impervious surfaces at the Kabailia Lakhder site, which influences its ability to carry out processes such as dry deposition and microclimate regulation. Overall, the data presented in Table 5 characterize the variation in multilayered vegetation between the three designs, thus establishing the structural basis for their respective potential for fine particle capture and CO_2 reduction.

Regarding the evaluation of vegetation vigor, this study clarifies that the NDVI values recorded across the studied gardens range primarily between 0.3 and 0.4 (Fig. 2), with localized peak areas reaching 0.5. While these values fall within a range common to many urban environments, they are interpreted herein as an indicator of "latent ecological capacity" rather than absolute structural failure.

It is essential to distinguish between NDVI, a spectral measure of chlorophyll activity and plant health, and leaf area index (LAI), which represents the three-dimensional structural density critical for aerodynamic pollutant capture. The relationship between NDVI and LAI is established as nonlinear; spectral indices like NDVI tend to saturate at moderate biomass levels, whereas LAI continues to provide a more accurate metric for the physical surface area available for dry deposition and wind-flow modification. For the quantitative support for the transition from spectral observations to structural modeling, the baseline leaf area index (LAI) was derived from observed normalized difference vegetation index (NDVI) values. This was achieved using an empirical exponential relationship established for Mediterranean vegetation, following the approach validated in similar environments (Fan et al., 2009; Padró et al., 2019) $\mathrm{LAI} = a.e^{b.\mathrm{NDVI}}$.

Within the ENVI-met simulation framework, the observed NDVI (Fig. 2) values (0.3–0.5) served as a baseline to inform the initial biological health parameters. However, the subsequent pollutant mitigation

Table 4 Concentrations of CO_2 measured by ENVI-met each 2 h in the three gardens in 4 days

	CO_2 ppm data/time of simulation	Day 1	Day 2	Day 3	Day 4
Ben Mihoub Hassen Garden					
Station A	8:00 AM	358	348	353	360
	10:00 AM	364	358	362	359
	12:00 AM	418	413	414	419
	2:00 PM	368	348	363	370
	4:00 PM	457	438	443	458
	6:00 PM	456	448	453	457
	8:00 PM	420	411	415	418
Station B	8:00 AM	350	338	343	351
	10:00 AM	348	328	343	345
	12:00 AM	410	406	409	410
	2:00 PM	353	348	351	354
	4:00 PM	455	454	453	451
	6:00 PM	456	355	453	386
	8:00 PM	420	418	419	421
Station C	8:00 AM	348	331	341	353
	10:00 AM	346	334	344	348
	12:00 AM	406	382	383	409
	2:00 PM	341	328	339	349
	4:00 PM	454	473	460	483
	6:00 PM	453	438	443	454
	8:00 PM	410	406	347	453
Station D	8:00 AM	314	310	313	318
	10:00 AM	328	318	323	333
	12:00 AM	378	379	381	383
	2:00 PM	328	318	323	332
	4:00 PM	410	409	406	413
	6:00 PM	406	386	390	410
	8:00 PM	386	368	373	388
Station E	8:00 AM	348	353	350	358
	10:00 AM	353	354	357	364
	12:00 AM	398	390	393	403
	2:00 PM	331	350	340	350
	4:00 PM	463	473	462	473
	6:00 PM	453	476	473	458
	8:00 PM	407	333	353	413

Table 4 (continued)

	CO_2 ppm data/time of simulation	Day 1	Day 2	Day 3	Day 4
Les Frères Boulmokh Garden					
Station A	8:00 AM	360	350	355	362
	10:00 AM	366	360	364	361
	12:00 AM	420	415	416	421
	2:00 PM	370	350	365	372
	4:00 PM	459	440	445	460
	6:00 PM	458	450	455	459
	8:00 PM	422	413	417	420
Station B	8:00 AM	352	340	345	353
	10:00 AM	350	330	345	347
	12:00 AM	412	408	411	412
	2:00 PM	355	350	353	356
	4:00 PM	457	456	455	453
	6:00 PM	458	357	455	388
	8:00 PM	422	420	421	423
Station C	8:00 AM	350	333	343	355
	10:00 AM	348	336	346	350
	12:00 AM	408	384	385	411
	2:00 PM	343	330	341	351
	4:00 PM	456	475	462	485
	6:00 PM	455	440	445	456
	8:00 PM	412	408	349	455
Station D	8:00 AM	316	312	315	320
	10:00 AM	330	320	325	335
	12:00 AM	380	381	383	385
	2:00 PM	330	320	325	334
	4:00 PM	412	411	408	415
	6:00 PM	408	388	392	412
	8:00 PM	388	370	375	390
Station E	8:00 AM	350	355	352	360
	10:00 AM	355	356	359	366
	12:00 AM	400	392	395	405
	2:00 PM	333	352	342	352
	4:00 PM	467	475	464	475
	6:00 PM	457	478	475	460
	8:00 PM	411	335	355	415
Kabailia Lakhder Garden					
Station A	8:00 AM	350	340	345	352
	10:00 AM	356	350	354	351
	12:00 AM	410	405	406	411
	2:00 PM	360	340	355	362
	4:00 PM	449	430	435	450
	6:00 PM	448	440	445	449
	8:00 PM	412	403	407	410

Table 4 (continued)

	CO_2 ppm data/time of simulation	Day 1	Day 2	Day 3	Day 4
Station B	8:00 AM	342	330	335	343
	10:00 AM	340	320	335	337
	12:00 AM	402	398	401	402
	2:00 PM	345	340	343	346
	4:00 PM	447	446	445	443
	6:00 PM	448	347	445	378
	8:00 PM	412	410	411	413
Station C	8:00 AM	340	323	333	345
	10:00 AM	338	326	336	340
	12:00 AM	398	374	375	401
	2:00 PM	333	320	331	341
	4:00 PM	446	465	452	475
	6:00 PM	445	430	435	446
	8:00 PM	402	398	339	445
Station D	8:00 AM	306	302	305	310
	10:00 AM	320	310	315	325
	12:00 AM	370	371	373	375
	2:00 PM	320	310	315	324
	4:00 PM	402	401	398	405
	6:00 PM	398	378	382	402
	8:00 PM	378	360	365	380
Station E	8:00 AM	340	345	342	350
	10:00 AM	345	346	349	356
	12:00 AM	390	382	385	395
	2:00 PM	323	342	332	342
	4:00 PM	457	465	454	465
	6:00 PM	447	468	465	450
	8:00 PM	401	325	345	405

analysis is fundamentally driven by the simulated LAI and crown morphology, which govern the mechanical processes of particle interception. The literature supports this distinction, noting that while NDVI reflects photosynthetic potential and biomass vigor, the actual efficiency of $PM_{2.5}$ and CO_2 reduction is more directly correlated with structural complexity and total leaf surface area (Nowak et al., 2014).

ENVI-met model calibration and validation

The high statistical agreement observed in this study ($d > 0.99$) is attributable to the resolution and quality

Table 5 The diversified green ratios for the three gardens

The garden's name	Total tree canopy surface	Total garden's surface	Urban forest index	Grass area (m^2)	Shrub area (m^2)	Total area (m^2)	Grass ratio (%)	Shrub ratio (%)	Total vegetation (%)
Kabailia Lakhder	1835.11	8437.638	21.75%	165.85	216.004	8437.638	1.96%	2.56%	4.5%
Les Frères Boulmokh	3486.061	9597.224	36.32%	1268.36	1056.436	9597.224	13.2%	11.0%	24.2%
Ben Mihoub Hassen	3634.476	11,962.428	30.38%	1310.473	1724.16	11,962.428	11.0%	14.4%	25.4%

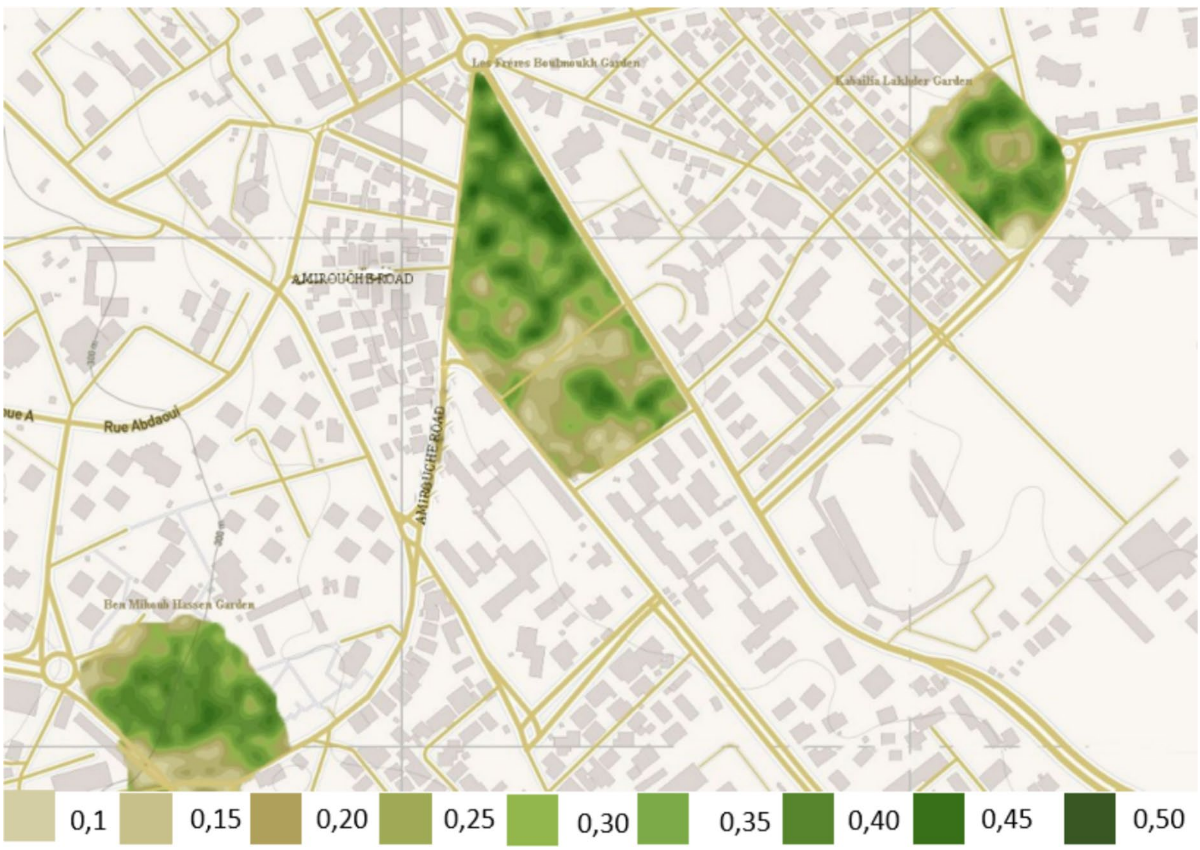

Fig. 2 Normalized difference vegetation index (NDVI) obtained from the study area. Taken from the open-access web EO Browser (https://apps.sentinel-hub.com/eo-browser/)

of input data used to initialize the ENVI-met environment. Rather than relying on generalized regional meteorological station data which may inadequately represent microclimatic variability within heterogeneous urban fabrics, the model was configured using a full simple forcing strategy. This approach utilized hourly air temperature, relative humidity, and background pollutant concentrations ($PM_{2.5}$ and PM_{10}) derived from in situ field measurements recorded during the 4-day study period (Fig. 3). The study employed strict separation of calibration and validation datasets: Data from the initial 24-h cycle were used for model calibration through boundary condition forcing, while independent observations from the subsequent three days comprising 72 paired hourly observations per site ($n = 216$ total) were reserved for statistical validation. Temporal alignment was achieved through synchronization of the model's 60-min output intervals with physical datalogger timestamps.

Field measurements were conducted using a PCE-MPC 20 Air Sampler, which features a PM measurement resolution of 1 μg/m^3 and a manufacturer-specified instrumental uncertainty of ± 10%. For fine particulate matter ($PM_{2.5}$), the model consistently reproduced temporal dynamics across all sites, as indicated by an R^2 value approaching 1.00. However, residual error analysis revealed localized systematic offsets that varied by location: Kabailia Lakhder Garden exhibited a mean absolute error (MAE) of 4.29 μg/m^3 and root mean square error (RMSE) of 4.63 μg/m^3, while Jardin Boulmokh and Jardin Ben Mihoub showed convergence between MAE and RMSE at 2.00 μg/m^3 and 5.00 μg/m^3, respectively. This convergence indicates the presence of constant systematic bias in model output specifically, a negative offset of − 2 μg/m^3 at Jardin Boulmokh and a positive offset of + 5 μg/m^3 at Jardin Ben Mihoub. These offsets fall within the ± 10% instrumental uncertainty range of the PCE-MPC 20 device, and the high R^2 value confirms that these discrepancies represent consistent linear shifts rather than stochastic error. Consequently, while quantifiable offsets exist, the model effectively simulates relative temporal patterns and variability of $PM_{2.5}$ concentrations throughout the study period.

Efficacy of design scenarios on PM concentrations

The modeling phase seeks to explore the potential influence of biophilic design on particulate matter concentrations. Particular attention is given to vegetative parameters, with the aim of investigating whether attributes such as density, type, diversity, or placement of green cover may have a larger effect on air quality besides water features or ground surface materials. To support this exploration, six individual scenarios (S1–S6) are proposed. Each scenario is assigned a tentative identifier and described in Table 2, along with its key parameters and associated parameterization tables. An overview of these scenarios is provided below.

S1—increased green cover density
S2—diversified green cover
S3—water features
S4—reconfiguration of vegetation placement
S5—modification of vegetation type
S6—modification of ground surface materials

In addition, combined scenarios are simulated to examine whether applying multiple interventions together could yield further reductions in pollutant concentrations. Each combined scenario is tentatively defined as a combination of individual scenarios.

Scenario S1 (increased green cover coverage) explores whether elevating the urban forest index to a target of 60% may address the identified biomass deficit. This densification is simulated to examine the potential impact of maximizing the leaf area index (LAI) on the removal of $PM_{2.5}$ and PM10 via dry deposition, as well as the possible increase in CO_2 reduction.

Scenario S2 (diversified green cover) investigates whether introducing complete vegetative stratification could expand upon quantitative increases in green cover. This simulation integrates dense shrub and herbaceous layers alongside specific tree species recognized for their pollutant-capture efficacy, including *Platanus × acerifolia*, *Acer saccharinum*, and *Quercus* spp. This multilayered approach is explored for its potential to increase surface roughness, disrupt airflow, and enhance particulate interception across vertical strata.

Scenario S3 (water features) is simulated to explore the extent to which aquatic elements may contribute to reducing ambient airborne particulate matter (Table 6).

Scenario S4 (reconfiguration of vegetation placement) examines whether applying principles of aerodynamic urbanism specifically, strategically repositioning vegetation to interact with prevailing winds could enhance pollutant interception and dispersion.

Scenario S5 (modification of vegetation type) explores the potential impact of altering biomass morphology by substituting existing low-LAI species (e.g., palms) with species characterized by higher foliage density, including *Platanus × acerifolia*, *Acer saccharinum*, and *Quercus* spp. This taxonomic substitution is simulated to investigate whether complex foliar morphology and higher LAI may enhance

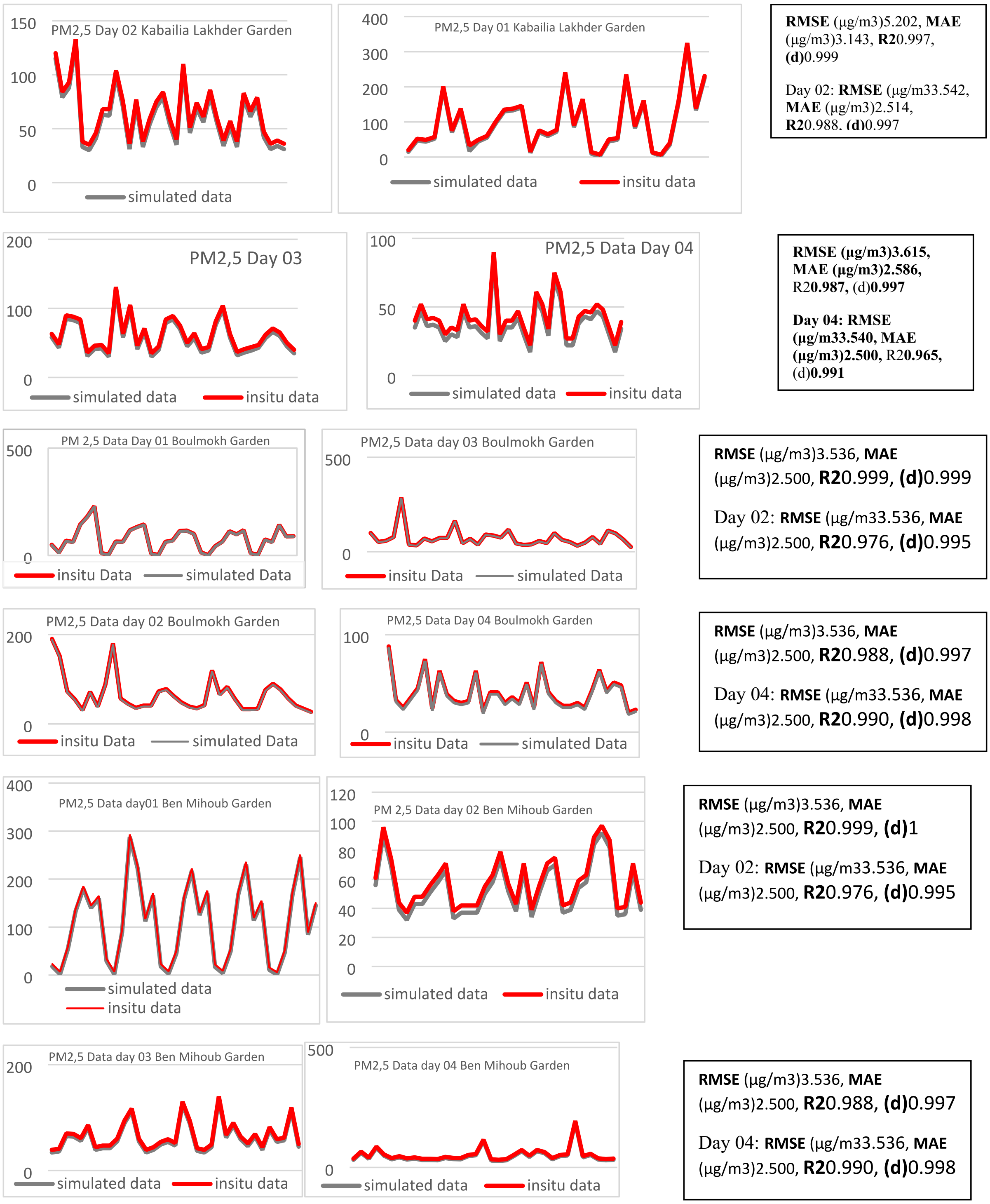

Fig. 3 Temporal validation of modeled $PM_{2.5}$ concentrations at the studied gardens. Time-series plots for four consecutive days show the comparison between ENVI-met simulated data (gray line) and in situ measured data (red line). Daily performance metrics (root mean square error [RMSE], mean absolute error [MAE], and coefficient of determination [R^2]) are annotated on each subplot. The high R^2 values ($\geq$0.976) and low error metrics demonstrate the model's strong capability in replicating the temporal dynamics of $PM_{2.5}$ concentrations. Source: authors (2025)

Table 6 The combined factors simulations' results in the three gardens

Garden/urban context	Optimal scenario combination	Key performance indicators and maximum reduction	Proposed design framework (based on model outcomes)
1. Kabailia Lakhder Garden (baseline/low efficiency) *Context: dispersed, high pollution load*	Combined package: • S1: increased green cover density • S2: diversified green cover • S5: modification of vegetation type • S6: modification of ground surface materials	Maximum reduction achieved: • $PM_{2.5}$: 78.4% (72.29 → 15.60 µg/m^3) • PM_{10}: 56.2% (104.45 → 45.80 µg/m^3) • CO_2: 7.9% (378.03 → 348.27 ppm) Performance insight: The comprehensive systemic overhaul is nonnegotiable for low-efficiency sites	Guideline 1: the 60/15/15 canopy formula For coarse-grained, polluted sites, achieve: • Urban forest index ≥ 60% with high-LAI trees (plane, maple, oak) • Multilayered stratification (tree + shrub + ground) • Soil roughness (z_0) ≥ 0.15 m on > 65% of site → This yields $PM_{2.5}$ reduction of ~ 75–80%
2. Boulmokh Garden (consolidated/medium efficiency) *Context: existing structure, moderate pollution*	Combined package: • S4: reconfiguration of vegetation placement • S2: diversified green cover • S3: water features (15% coverage)	Maximum reduction achieved: • $PM_{2.5}$: ~ 33.5% (75.21 → 49.99 µg/m^3) • PM_{10}: ~ 32.2% (145.45 → 98.80 µg/m^3) • CO_2: ~ 2.1% (390.86 → 382.87 ppm) Performance insight: Aerodynamic placement (S4) was the dominant lever here, surpassing species optimization (S5)	Guideline 2: the aerodynamic priority In consolidated fabrics, the spatial arrangement of existing biomass is more critical than adding more • Prioritize wind-corridor alignment of greenery • Use water features (~ 15% coverage) for humidification and deposition • Targeted infill over blanket canopy increase → This yields PM reduction of ~ 30–35%
3. Ben Mihoub Garden (compact/high efficiency) *Context: dense, favorable microclimate*	Combined package: • S5: modification of vegetation type • S6: modification of ground surface materials • S2: diversified green cover	Maximum reduction achieved: • $PM_{2.5}$: ~ 19.7% (80.92 → 64.99 µg/m^3) • PM_{10}: ~ 17.8% (95.41 → 78.45 µg/m^3) • CO_2: 10.15% (387.63 → 348.27 ppm) Performance insight: Carbon concentration mitigation excels (S5), but PM reduction is limited. Focus on space-efficient, high-performance species	Guideline 3: the carbon-first vertical strategy In compact cores, maximize sequestration per m^2 • Deploy high-LAI vertical species (ivy, bamboo, fast-growing conifers) • Convert > 40% of impervious courtyards to planted beds • Use pollutant-absorbing materials on remaining surfaces → This yields CO_2 reduction > 10% with ~ 20% PM cobenefit

particulate capture and provide improved thermal regulation within the urban canopy (Fig. 4).

Scenario S6 (modification of ground surface materials) simulates the potential effect of replacing impervious and mineral surfaces with permeable alternatives, such as stabilized permeable pavements and biophilic mulch. The key mechanistic parameter in this exploratory simulation is the aerodynamic roughness length (z_0), provisionally adjusted to 0.15 m. This increase in surface roughness is explored for its potential to enhance near-ground air friction and localized turbulence, which may promote the interception and sedimentation of particulate matter by reducing its advective transport (Fig. 4).

Discussion

Initial simulation results (the temporal evolution of $PM_{2.5}$, PM10, and CO_2 for all scenarios is

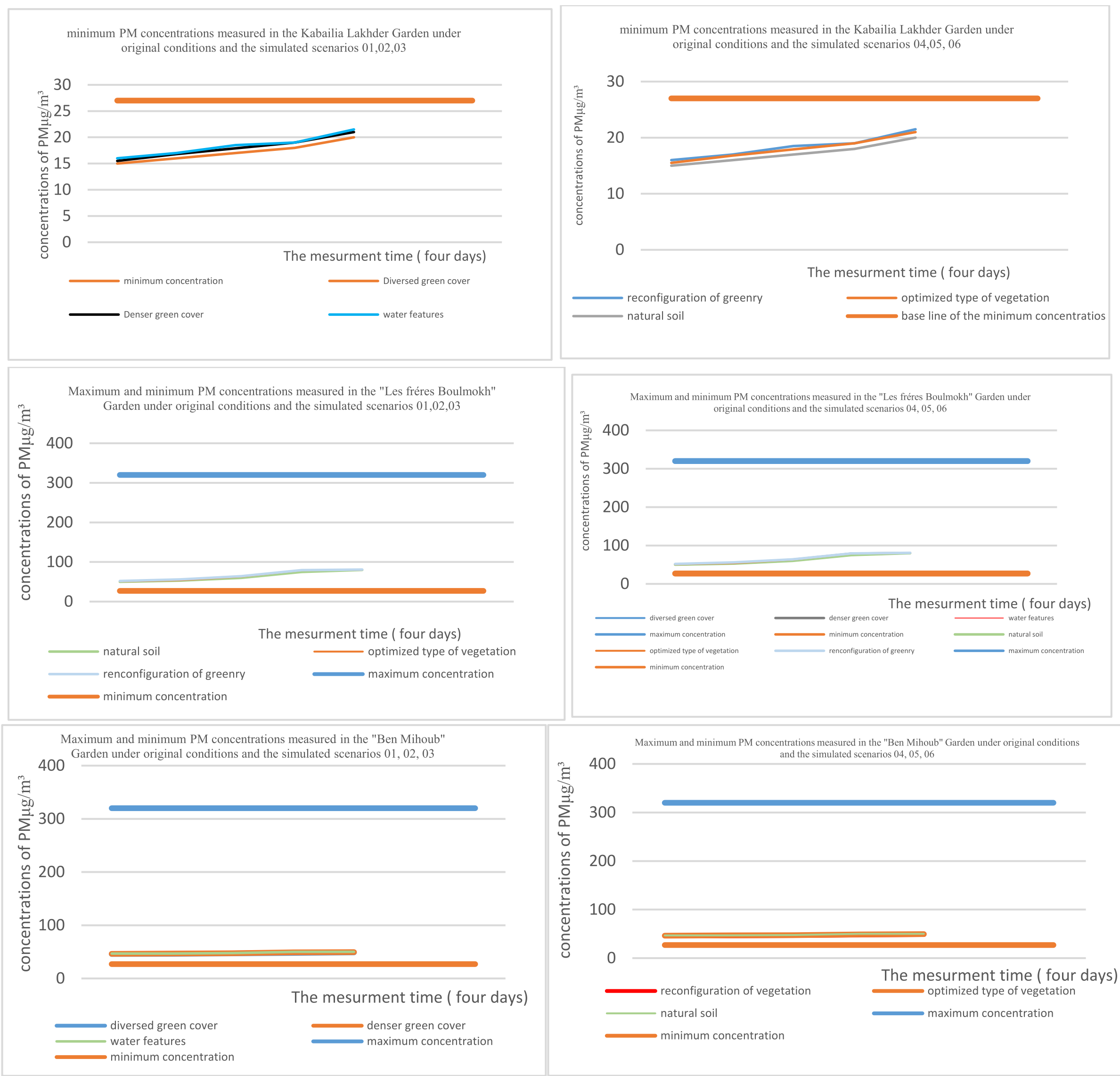

Fig. 4 Comparison of six simulated scenarios (average values), against daily baseline concentrations across all study sites. Source: authors 2025

illustrated in Figs. 4 and 5; for a precise quantitative comparison, the full numerical datasets at 2-h intervals are provided in the Supplementary Information (Tables 6–9)) for the high-exposure site indicate persistently elevated particulate matter concentrations, with relatively slight performance differentiation among the initial intervention scenarios (e.g., dense vs. diversified canopy). These data suggest that, under the specific summer meteorological conditions modeled, strategies focused primarily on increasing the volumetric density of greenery or incorporating aquatic elements (while common in urban greening) may yield diminishing returns when subjected to substantial urban pollution fluxes. This observation is significant, as it underscores the importance of moving beyond purely quantitative vegetation provision toward a design approach that integrates specific aerodynamic and biochemical mechanisms governing pollutant capture within high-traffic contexts.

Subsequent analysis indicates that the selection of vegetation functional types (Scenario 05) represents a significant variable for localized air quality improvement. In the modeled environments, this scenario consistently demonstrated higher mitigation potential for $PM_{2.5}$ (Fig. 4), PM10, and CO_2 compared to spatial reconfiguration alone (Scenario 04). These findings support the hypothesis of a bottom-up approach, suggesting that intrinsic plant properties such as foliar morphology and leaf area index may be more influential predictors of intervention performance than structural layout or the addition of ancillary elements like water features and engineered soils within these specific urban configurations (Fig. 5).

The simulated CO_2 concentration results align with this hierarchy of effectiveness, though the magnitude of reduction was less pronounced than for particulate matter. This discrepancy is likely attributable to the dual nature of CO_2 mitigation, which involves both atmospheric dispersion and simulated biological uptake. While CO_2 was not measured in the field campaign, these modeled results are presented as exploratory indicators of how design changes might influence gas concentrations (Fig. 5). Consistent with the PM findings, the optimized vegetation type scenario (Scenario 05) maintained the lowest CO_2 concentrations. This convergence suggests that targeted

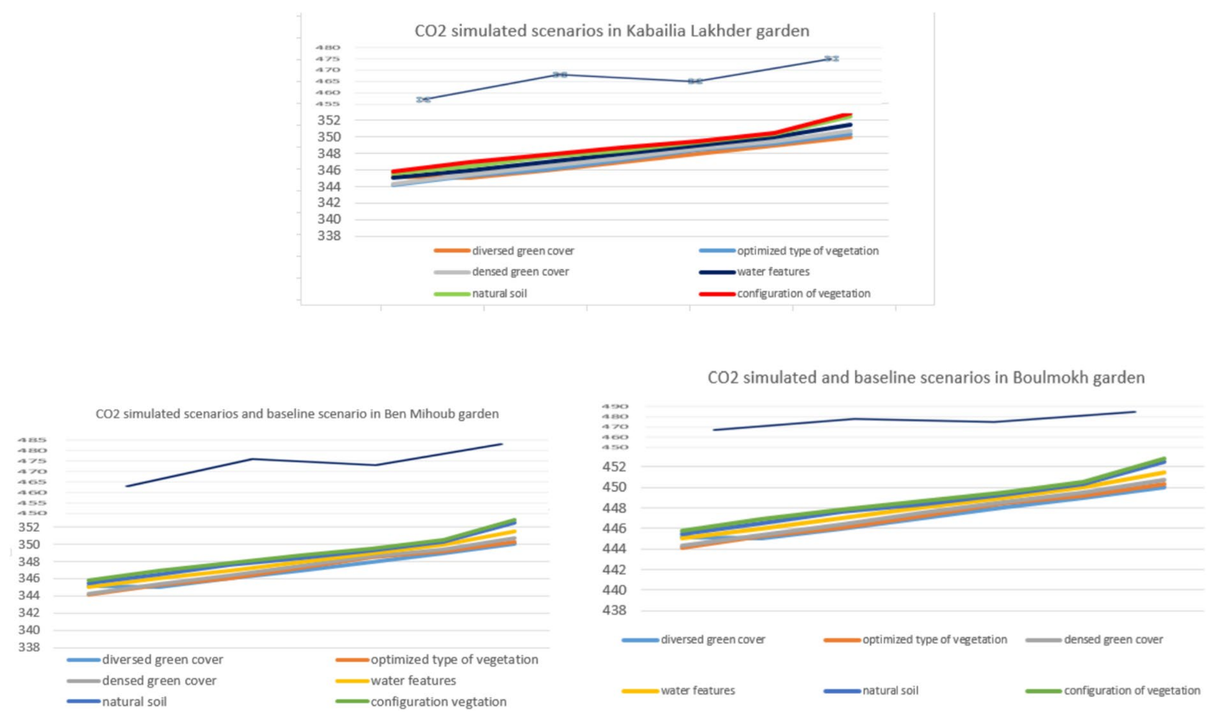

Fig. 5 Comparison of six simulated scenarios of CO_2 (average values), against daily baseline concentrations across all study sites. Source: authors 2025

biophilic strategies may generate synergistic cobenefits, although the absolute magnitude of these reductions remains contingent upon the model's internal biological assumptions and background boundary conditions.

Analysis of the initial scenarios (01, 02, 03) suggests that specific vegetation types may yield the highest mitigation efficacy, indicating species selection as a key predictive factor. A more granular examination of the advanced design scenarios (04, 05, 06) reveals a notable nuance: The performance curves for denser green cover and water features are nearly superimposed, both exhibiting marginally higher pollution levels than the diversified green cover scenario. This indicates that, within the specific microclimatic context of Jardin de Boulmokh, interventions focused solely on increasing canopy density or introducing aquatic elements may not significantly alter localized concentration fields of $PM_{2.5}$ or CO_2. Therefore, within the limited microclimatic context of Jardin de Boulmokh during the study period model, mitigation efficacy appears to be less a function of biomass quantity or the presence of water features and is instead influenced more directly by strategic taxonomic selection.

Findings of scenarios for Jardin Ben Mihoub suggest a distinct determinant of efficacy. Within this specific simulation, the reconfiguration of vegetation (Scenario 04) exhibited the highest performance for PM reduction, exceeding the optimized vegetation type (Scenario 05). A potential functional trade-off is indicated through the exploratory analysis of CO_2. While Scenario 05 maintains the lowest CO_2 levels, a result driven by the model's assumptions regarding species-specific physiology, the reconfiguration scenario ranks lower for CO_2 mitigation despite its PM efficacy. This divergence suggests that an aerodynamic design optimized for particulate dispersion is not necessarily congruent with one optimized for lowering CO_2 concentrations. Given that explicit carbon flux accounting was not conducted, these CO_2 findings remain assumption-dependent and emphasize the complexity of multipollutant mitigation in unmeasured atmospheric fields.

Synthesis: multifactor impact on pollutant reduction

Modeling a composite biophilic intervention integrating increased vegetation density, stratified diversity, high-efficiency species, water features, and modified soil properties reveals a complex, context-dependent impact on atmospheric pollutants. The results, under the simulated conditions, demonstrate a pronounced and consistent reduction in particulate matter ($PM_{2.5}$ and PM_{10}) across the studied gardens. In contrast, the response of carbon dioxide (CO_2) was more variable and of a generally lower magnitude. This divergence reflects the distinct mechanistic pathways governing the removal of particulate pollution (primarily through dry deposition and aerodynamic effects) versus carbon reduction as summarized in Table 5.

The efficacy of the composite intervention was notably context-dependent. The most significant PM reductions were observed at Kabailia Lakhder Garden "baseline, low efficiency," with simulated decreases of 78.4% for $PM_{2.5}$ and 56.15% for PM10. This relative performance is attributed to the site's favorable initial morphology, characterized by greater openness that appears to have facilitated enhanced air circulation and the more effective dispersion and interception of particles by the introduced vegetation. In contrast, the interventions yielded more moderate PM reductions at Jardins Les Frères Boulmokh "consolidated/medium efficiency" (33.5% for $PM_{2.5}$) and Ben Mihoub Hassen "compact/high efficiency" (19.7% for $PM_{2.5}$). This performance disparity highlights the influence of extrinsic, site-specific factors. At Les Frères Boulmokh, proximity to high-traffic corridors generated a constant influx of emissions that may have saturated the mitigation capacity of the vegetation. For Ben Mihoub Hassen, the pre-existing dense vegetation and a potentially more enclosed urban fabric likely limited the marginal gain of additional interventions and restricted pollutant dispersion through ventilative flushing, resulting in a potential containment effect. These findings, for the studied period, suggest that the existing urban morphology, including its openness and interaction with wind patterns, is a primary factor governing the efficacy of particulate matter mitigation strategies.

In the specific context of high-temperature summer days, the composite intervention yielded significantly lower and more variable reductions in CO_2 concentrations (ranging from 2.05 to 10.15%) compared to those achieved for particulate matter (Table 5). This discrepancy stems from the fundamental difference in their removal mechanisms. Particulate matter is mitigated through immediate physical processes dry deposition and impaction which are directly enhanced by increasing vegetative surface area and aerodynamic roughness. In contrast, CO_2 removal is a long-term biochemical process dependent on photosynthetic concentration mitigation, a function constrained by total biomass and growth rates.

The simulated modest reductions indicate that while the intervention establishes a foundational carbon sink, its full concentration mitigation potential would likely be realized progressively as the plant community matures. The relatively higher performance observed in the model at Ben Mihoub Hassen Garden (10.15% reduction) may be attributed to its pre-existing high vegetation density; the introduction of high-efficiency species served to potentially optimize an already substantial photosynthetic baseline, yielding a more pronounced marginal gain within the simulation parameters.

To address the practical feasibility of achieving the proposed 60% urban forest index, this study reframes the target from a static design objective to a phased dynamic implementation framework structured across three temporal horizons: an establishment phase (0–5 years) focused on understory vegetation for immediate microclimatic benefits, a consolidation phase (5–15 years) characterized by increasing leaf area index (LAI) and the progressive enhancement of carbon concentration mitigation and particulate matter (PM) filtration, and a maturity phase (15–30 + years), where full biomass development allows the 60% urban forest index target to reach its maximum ecological expression (Table 6).

This longitudinal approach accounts for the nonlinear progression of ecosystem services, acknowledging that the 60% urban forest index corresponds to a specific densification scenario aimed at maximizing canopy coverage within the available spatial envelope. To resolve potential conflicts between high vegetation density and urban spatial functionality, a vertical-horizontal layering strategy is proposed, integrating vertical greening on adjacent facades and utilizing high-canopy, “lifted” tree structures to optimize biomass volume without encroaching upon pedestrian circulation or social activity zones (Table 6).

By anchoring the urban forest index target within this phased growth model and prioritizing strategic vertical placement, the framework transforms a theoretically optimal index into a viable, actionable planning roadmap that balances operational constraints such as maintenance and land-use trade-offs with the requirement for long-term ecological resilience in the Mediterranean urban context of Guelma (Table 6).

Contribution analysis and ranking of intervention leverage

To isolate the individual contributions of the biophilic interventions for this specific period and meteorological conditions, a comparative analysis of Scenarios 01 through 06 was conducted across all study sites. This decomposition reveals that the mitigation of particulate matter (PM) and the concentration mitigation of carbon dioxide (CO_2) are governed by a clear hierarchy of drivers, with aerodynamic reconfiguration and canopy density emerging as the primary levers of performance within the study context.

The simulation data indicate that canopy densification (Scenario 01) and aerodynamic reconfiguration (Scenario 04) consistently yielded the most significant reductions in pollutant concentrations. In the Kabailia Lakhder garden, which exhibited the highest overall percentage gains, the densification of the canopy acted as the primary driver by substantially increasing the deposition surface area and modifying local airflow patterns. This confirms that aerodynamic effects specifically the generation of turbulence and the reduction of wind speed through enhanced structural roughness constitute the most influential factors in capturing $PM_{2.5}$ and PM_{10}. Consequently, the primary driver for air quality improvement identified in this methodological framework in this study is the physical structure and density of the vegetation, rather than its specific biological classification.

The secondary driver identified is the optimized selection of vegetation type (Scenario 05). While the introduction of high-efficiency species provided measurable improvements, the magnitude of these gains was secondary to those achieved by density and aerodynamic reconfiguration alone. This suggests that although biological traits such as leaf surface texture and stomatal characteristics enhance filtration efficiency, they cannot compensate for insufficient total biomass within the simulated environment. It should be noted that the perceived impact of these traits on CO_2 remains exploratory, as the model primarily calculates concentration shifts rather than long-term carbon assimilation.

Diversified green cover (Scenario 01) and engineered soil modification (Scenario 06) provided moderate tertiary benefits, primarily by stabilizing the microclimate and reducing ground-level particle resuspension. However, these interventions exhibited the least impact on the overarching CO_2 and PM concentration curves. The limited response in CO_2 levels further underscores that, under these diurnal modeling assumptions, atmospheric dispersion driven by site morphology is the dominant factor influencing gas concentrations.

Notably, water features (Scenario 03) demonstrated variable effectiveness; while beneficial for thermal cooling through evaporative processes, their contribution to particulate matter reduction remained marginal compared to vegetative interventions.

Conclusion

This study employed an integrated monitoring and modeling approach to evaluate the potential effectiveness of biophilic design in mitigating atmospheric pollutants across three urban gardens in Guelma, Algeria. The findings of the studied period and specific meteorological conditions suggest that the performance of green infrastructure is not simply a function of vegetation quantity but is largely determined by site-specific design parameters. While interventions based solely on increasing generic green cover produced only marginal benefits within the model, the strategic selection of high-efficiency plant species (optimized vegetation type) emerged as a significant factor in reducing PM and enhancing CO_2 concentration mitigation in two of the three sites. In the third garden, however, the spatial reconfiguration of vegetation to interact with local wind flows was indicated as the dominant factor in PM attenuation.

A key observation from this assessment is the potential functional divergence between optimal design for particulate matter filtration and for carbon dioxide concentration mitigation. This divergence highlights the importance of moving beyond one-size-fits-all greening strategies. Instead, the results provide support for a performance-based design framework, informed by microclimate modeling, which emphasizes spatial configuration for immediate PM control and taxonomic selection for long-term carbon cycling.

While the findings are derived from an exploratory analysis based on a specific 4-day summer field campaign and a single diurnal simulation cycle, they offer a preliminary understanding of how combined biophilic interventions can demonstrate significant potential for immediate mitigation of particulate pollution. Under these specific meteorological conditions, their success was strongly linked to local urban morphology and proximity to emission sources. For CO_2, these strategies represent a long-term investment, with concentration mitigation rates dependent on vegetative maturation. Consequently, within the limits of this temporal scope, this research suggests that effective urban air quality management benefits from a pollutant-specific and context-sensitive assessment methodology. While further multiseasonal validation is required to support generalized design standards, these results illustrate that optimizing the ecosystem services of urban green spaces requires designs informed by the unique microclimatic and anthropogenic pressures of each site, aiming for measurable and sustainable improvements in urban environmental quality.

Research limits

The present study acknowledges several methodological constraints that should be considered when interpreting the results. First, the temporal scope of the simulations represents a specific diurnal cycle; however, air quality parameters particularly CO_2 concentration mitigation require long-term longitudinal evaluation to establish definitive guidelines for urban design. Second, the current model does not fully account for stochastic meteorological variations, such as seasonal weather shifts and fluctuating wind gustiness, which are critical determinants of pollutant dispersion and concentration levels.

The CO_2 concentrations were not physically measured during the field campaign; consequently, the simulated ppm reductions should not be equated with absolute biological carbon sequestration. As explicit flux accounting was not conducted, these results are best interpreted as exploratory and assumption-dependent indicators of how vegetation influences local concentration fields, rather than as absolute predictions of carbon uptake. This is further contextualized by the inherent simplifications of the ENVI-met

CO_2 module, which is designed to simulate local-scale variations driven by vegetation and primary emission sources but does not account for advection from distant regional sources or complex atmospheric chemistry. Additionally, while traffic emissions were explicitly modeled using updated data from the transport administration, the software utilizes simplified emission factors rather than complex combustion chemistry. Temporal resolution also presents a constraint, as the simulation, while suitable for capturing diurnal patterns, may not resolve rapid, instantaneous fluctuations caused by sudden changes in traffic turbulence or microscale gusts.

While the simulated scenarios demonstrate a substantial reduction in particulate matter (PM), reaching up to 78% in localized areas, these findings must be interpreted within the specific context of the 4-day summer monitoring period. The observed mitigation levels are closely associated with the stable atmospheric conditions and prevailing wind patterns primarily from the northwest recorded during the field campaign in Guelma. Under different seasonal conditions, such as winter periods marked by increased atmospheric stability or altered wind directions, the dispersion and deposition dynamics of particulate matter may vary considerably.

To address these limitations, it is recommended that future research utilize comprehensive multisensor monitoring stations capable of synchronized data acquisition for both meteorological and pollutant parameters. Establishing a robust empirical baseline through simultaneous field measurements of wind velocity, temperature, and pollutant flux is essential for the subsequent calibration and validation of microscale simulation models. Such an integrated approach would enhance the predictive accuracy of biophilic design interventions across varying climatic scenarios.

Acknowledgements I would like to express my sincere and deepest gratitude to Professor Alkama Djamel for his unwavering support, constant encouragement, and generous allocation of his time were essential for the successful completion of this project. His commitment to academic excellence serves as a continuous source of inspiration.

Author contribution All authors contributed equally to the conception, execution, data analysis, and manuscript preparation of this research, sharing all procedures and research work equivalently. Specifically, Rayen Bechlem led the efforts on the initial drafting and site investigation; Fatima Zahra Djouad performed the critical review and corrected the final version; Boudjehem Hocine managed the data collection and ensured software availability; and Hana Salah-Salah was instrumental in building the methodology and the referential framework.

Funding This work received no funding.

Data availability All data generated or analyzed during this study are included in this published article [and its supplementary information files].

Declarations

Competing interests The authors declare no competing interests.

References

Acierno, A., & Coppola, E. (n.d.). Green blue infrastructure methodologies and design proposals. SHARE Libri. Retrieved May 15, 2026, from http://www.fedoabooks.unina.it/index.php/fedoapress/catalog/view/344/379/1935

Aimar, S., Mendez, M., Funk, R., & Buschiazzo, D. (2012). Soil properties related to potential particulate matter emissions (PM10) of sandy soils. *Aeolian Research*. https://doi.org/10.1016/j.aeolia.2010.12.001

Beatley, T., & Newman, P. (2013). Biophilic cities are sustainable, resilient cities. *Sustainability*. https://doi.org/10.3390/su5083328

Bechlem, R., Djouad, F. Z., Debbache, A., & Salah-Salah, H. (2025). Weaving nature into the urban tapestry: Biophilic design, public spaces, and identity in the city. In G. Hayder, M. Fairuz Shahidan, & A. Ozcan-Buckley (Eds.), *Cities' Identity Through the Art of Urban Spaces* (pp. 37–43). Springer Nature Switzerland. https://doi.org/10.1007/978-3-031-94821-3_4

Bechlem, R., Djouad, F.-Z., & Salah-Salah, H. (2024). Morphological analysis of public spaces and their contribution to urban resilience in Guelma, Algeria. *Journal of Mediterranean Cities, 4*(1), 167–177. https://doi.org/10.38027/mediterranean-cities_vol4no1_10

Bouhallit, Z., Djouad, F. Z., Dechaicha, A., & Alkama, D. (2024). Assessment of the quality of public garden use through their urban furniture, case study of the city of Guelma, Algeria. *South Florida Journal of Development, 5*(12), e4844–e4844. https://doi.org/10.46932/sfjdv5n12-063

Boulekbache-Mazouz, H. (2008). Lire l'espace public pour mieux l'écrire. *Études de Communication*. https://doi.org/10.4000/edc.757

Bouznit, M., & Pablo-Romero, MdelP. (2016). CO2 emission and economic growth in Algeria. *Energy Policy, 96*, 93–104. https://doi.org/10.1016/j.enpol.2016.05.036

Brulfert, G., Chollet, J.-P., Jouve, B., & Villard, H. (2005). Atmospheric emission inventory of the Maurienne Valley for an atmospheric numerical model. *Science of the Total Environment, 349*(1–3), 232–248. https://doi.org/10.1016/j.scitotenv.2005.01.013

Buccolieri, R., Gatto, E., Manisco, M., Ippolito, F., Santiago, J. L., & Gao, Z. (2020). Characterization of urban greening in a district of Lecce (Southern Italy) for the analysis of CO2 storage and air pollutant dispersion. *Atmosphere, 11*(9), Article 967.

Djouad, F. Z. (2021). The biophilic approach to qualify the inhabitant-nature relationship in the domestic space: The case of the City of El Kala, Algeria. *Architecture and Urban Planning, 17*(1), 103–111. https://doi.org/10.2478/aup-2021-0010

Dong, H., Chen, Y., Huang, X., & Cheng, S. (2023). Multi-scenario simulation of spatial structure and carbon sequestration evaluation in residential green space. *Ecological Indicators, 154*, Article 110902. https://doi.org/10.1016/j.ecolind.2023.110902

Du, H., Zhou, F., Cai, Y., Li, C., & Xu, Y. (2021). Influence of features of green spaces on health and well-being: Case study of Shanghai, China. *Journal of Urban Planning and Development, 147*(2), Article 04021008. https://doi.org/10.1061/(ASCE)UP.1943-5444.0000671

Fan, L., Gao, Y., Brück, H., & Bernhofer, C. (2009). Investigating the relationship between NDVI and LAI in semi-arid grassland in Inner Mongolia using in-situ measurements. *Theoretical and Applied Climatology, 95*(1–2), 151–156. https://doi.org/10.1007/s00704-007-0369-2

Fisher, B., Kukkonen, J., Piringer, M., Rotach, M. W., & Schatzmann, M. (2006). Meteorology applied to urban air pollution problems: Concepts from COST 715. *Atmospheric Chemistry and Physics, 6*(2), 555–564. https://doi.org/10.5194/acp-6-555-2006

Ge, W., & Zhang, G. (2022). Resilient public transport construction in mega cities from the perspective of ecological environment governance. *Journal of Environmental and Public Health, 2022*, 1–10. https://doi.org/10.1155/2022/9143618

Gebreyesus, T., Borgemeister, C., Herrero- Jáuregui, C., & Kelboro, G. (2024). Transforming urban air quality: Green infrastructure strategies for the urban centers of Ethiopia. *Environmental Pollution, 363*, Article 125244. https://doi.org/10.1016/j.envpol.2024.125244

Gehanno, J. F., Bonneterre, V., Andujar, P., Pairon, J. C., Paris, C., Petit, A., Verdun-Esquer, C., Durand-Moreau, Q., & Brochard, P. (2020). Arguments pour une possible transmission par voie aérienne du SARS-CoV-2 dans la crise COVID-19. *Archives des Maladies Professionnelles et de l'Environnement, 81*(4), 306–315. https://doi.org/10.1016/j.admp.2020.04.018

Godwin, C., Chen, G., & Singh, K. K. (2015). The impact of urban residential development patterns on forest carbon density: An integration of LiDAR, aerial photography and field mensuration. *Landscape and Urban Planning, 136*, 97–109. https://doi.org/10.1016/j.landurbplan.2014.12.007

Hu, M. (2017). Assessment of effective energy retrofit strategies and related impact on indoor environmental quality: A case study of an elementary school in the State of Maryland. *Journal of Green Building, 12*(2), 38–55. https://doi.org/10.3992/1943-4618.12.2.38

Jin, S., Stokes, G., & Hamilton, C. (2023). Empirical evidence of urban climate adaptation alignment with sustainable development: Application of LDA. *Cities, 136*, Article 104254. https://doi.org/10.1016/j.cities.2023.104254

Khaleghi, A., Bartlett, K., & Hodgson, M. (2011). Factors affecting ventilation, indoor-air quality and acoustical quality in 'green' and non-'green' buildings: A pilot study. *Journal of Green Building, 6*(3), 168–180. https://doi.org/10.3992/jgb.6.3.168

Khellaf, L., Ait-Aoudia, M. N., & Rahal, F. (2025). The CODASC database for analyzing the impact of morpho-climatic characteristics of canyon streets on the concentration of air pollutants. *Journal of Design for Resilience in Architecture and Planning, 6*(1), 102–123. https://doi.org/10.47818/DRArch.2025.v6i1159

Liu, H., Kobernus, M., & Liu, H. (2017). Public perception survey study on air quality issues in Wuhan, China. *Journal of Environmental Protection, 8*(10), Article Article 10. https://doi.org/10.4236/jep.2017.810075

Liu, J., Kamarudin, K. M., Liu, Y., & Zou, J. (2021). Developing pandemic prevention and control by ANP-QFD approach: A case study on urban furniture design in China communities. *International Journal of Environmental Research and Public Health, 18*(5), Article 2653. https://doi.org/10.3390/ijerph18052653

Muñoz-Pizza, D. M., Villada-Canela, M., Rivera-Castañeda, P., Reyna-Carranza, M. A., Osornio-Vargas, A., & Martínez-Cruz, A. L. (2020). Stated benefits from air quality improvement through urban afforestation in an arid city – A contingent valuation in Mexicali, Baja California, Mexico. *Urban Forestry & Urban Greening, 55*, Article 126854. https://doi.org/10.1016/j.ufug.2020.126854

Nowak, D. J., Hirabayashi, S., Bodine, A., & Greenfield, E. (2014). Tree and forest effects on air quality and human health in the United States. *Environmental Pollution, 193*, 119–129. https://doi.org/10.1016/j.envpol.2014.05.028

Padró, J.-C., Carabassa, V., Balagué, J., Brotons, L., Alcañiz, J. M., & Pons, X. (2019). Monitoring opencast mine restorations using unmanned aerial system (UAS) imagery. *Science of The Total Environment, 657*, 1602–1614. https://doi.org/10.1016/j.scitotenv.2018.12.156

Ramdane, M., Djouad, F. Z., Boumaza, O., & Salah-Salah, H. (2025). Assessment of the effect of the design of a public garden on the biophilic behavior of its users in Guelma (northeastern Algeria). *Urban Design International, 30*(3), 185–227. https://doi.org/10.1057/s41289-025-00280-9

Ramírez, O., Mura, I., & Franco, J. F. (2017). How do people understand urban air pollution? Exploring citizens' perception on air quality, its causes and impacts in Colombian cities. *Open Journal of Air Pollution, 6*(1), Article Article 1. https://doi.org/10.4236/ojap.2017.61001

Redondo Bermúdez, M., Chakraborty, R., Cameron, R. W., Inkson, B. J., & Val Martin, M. (2023). A practical green infrastructure intervention to mitigate air pollution in a UK school playground. *Sustainability, 15*(2), Article Article 2. https://doi.org/10.3390/su15021075

Ristianti, N. S., Dewi, S. P., Susanti, R., Kurniati, R., & Zain, N. S. (2024). Using biophilic design to enhance resilience of urban parks in Semarang City Indonesia Nakhara. *Journal of Environmental Design and Planning, 23*(1), 402. https://doi.org/10.54028/NJ20242340210.54028/NJ202423402

Rodrigues, V., Gama, C., Ascenso, A., Oliveira, K., Coelho, S., Monteiro, A., Hayes, E., & Lopes, M. (2021). Assessing air pollution in European cities to support a citizen centered approach to air quality management. *Science of the Total Environment, 799*, Article 149311. https://doi.org/10.1016/j.scitotenv.2021.149311

Shi, C., Guo, N., Gao, X., & Wu, F. (2022). How carbon emission reduction is going to affect urban resilience. *Journal of Cleaner Production, 372*, Article 133737. https://doi.org/10.1016/j.jclepro.2022.133737

Sjöblom, J., Ström, H., & Darnell, A. (2017). Characterization of particulate matter and the capture efficiency in open metal substrates. *Topics in Catalysis*. https://doi.org/10.1007/s11244-016-0622-y

Smieszek, M., Mateichyk, V., Dobrzanska, M., Dobrzanski, P., & Weigang, G. (2021). The impact of the pandemic on vehicle traffic and roadside environmental pollution: Rzeszow City as a case study. *Energies, 14*, Article 4299. https://doi.org/10.3390/en14144299

Tarek, S., & Ouf, A.-D. (2021). Biophilic smart cities: The role of nature and technology in enhancing urban resilience. *Journal of Engineering and Applied Science, 68*(1), Article 40. https://doi.org/10.1186/s44147-021-00042-8

VanOort, F., Jongmans, A. G., Lamy, I., Baize, D., & Chevallier, P. (2008). Impacts of long-term waste-water irrigation on the development of sandy Luvisols: Consequences for metal pollutant distributions. *European Journal of Soil Science, 59*(5), 925–938. https://doi.org/10.1111/j.1365-2389.2008.01047.x

Vigevani, I., Corsini, D., Mori, J., Pasquinelli, A., Gibin, M., Comin, S., Szwałko, P., Cagnolati, E., Ferrini, F., & Fini, A. (2022). Particulate pollution capture by seventeen woody species growing in parks or along roads in two European cities. *Sustainability, 14*(3), Article 1113. https://doi.org/10.3390/su14031113

Villani, M. G., Russo, F., Adani, M., Piersanti, A., Vitali, L., Tinarelli, G., Ciancarella, L., Zanini, G., Donateo, A., Rinaldi, M., Carbone, C., Decesari, S., & Sänger, P. (2021). Evaluating the impact of a wall-type green infrastructure on PM10 and NOx concentrations in an urban street environment. *Atmosphere, 12*(7), Article 839. https://doi.org/10.3390/atmos12070839

Wang, L., Niu, D., Fan, H., & Long, X. (2022). Urban configuration and PM2.5 concentrations: Evidence from 330 Chinese cities. *Environment International, 161*, Article 107129. https://doi.org/10.1016/j.envint.2022.107129

Willmott, C. J., Rowe, C. M., & Mintz, Y. (1985). Climatology of the terrestrial seasonal water cycle. *Abstract Journal of Climatology, 5*(6), 589–606. https://doi.org/10.1002/joc.3370050602

Zahra, D. F., Hana, S. S., Rayen, B., & Meriem, R. (2025). Biophilia: From a sociological and environmental theory to an urban and architectural approach. *Proceedings of the International Conference of Contemporary Affairs in Architecture and Urbanism-ICCAUA, 8*(1), 390–394. https://doi.org/10.38027/ICCAUA2025EN0036